The Oncolytic Activity of Myxoma Virus against Soft Tissue Sarcoma Is Mediated by the Overexpression of Ribonucleotide Reductase

Clinical Medicine Insights: Oncology
Volume 15: 1–7

DOI: 10.1177/1179554921993069
SAGE

Yanghee Woo[1,2], Susanne G Warner[1,2], Rula Geha[1], Marianne M Stanford[3], Penelope Decarolis[1,4], Masmudur M Rahman[5,6], Samuel Singer[1], Grant McFadden[5,6] and Yuman Fong[1,2]

[1]Department of Surgery, Memorial Sloan Kettering Cancer Center, New York, NY, USA. [2]Department of Surgery, City of Hope National Medical Center, Duarte, CA, USA. [3]Department of Microbiology & Immunology, Dalhousie University, Halifax, NS, Canada. [4]Department of Molecular Pharmacology, Albert Einstein College of Medicine, New York, NY, USA. [5]Department of Molecular Genetics & Microbiology, University of Florida, Gainesville, FL, USA. [6]Center for Immunotherapy, Vaccines and Virotherapy, Biodesign Institute, Arizona State University, Tempe, AZ, USA.

ABSTRACT

BACKGROUND: Myxoma virus (MYXV) is an oncolytic poxvirus that lacks the gene for 1 of the subunits of ribonucleotide reductase (RR), a crucial DNA synthesis and repair enzyme. The overexpression of RR has been implicated in the invasiveness of several cancers, including soft tissue sarcomas (STS). The purpose of the study was to investigate the oncolytic efficacy of MYXV in STS with different levels of RR expression.

METHODS: The oncolytic effect of recombinant MYXV was evaluated in 4 human STS cell lines, LS141 (a dedifferentiated liposarcoma), DDLS8817 (a dedifferentiated liposarcoma), RDD2213 (recurrent dedifferentiated liposarcoma), and HSSYII (a synovial sarcoma) using infectivity and cytotoxicity assays. Following the overexpression of RRM2 by cDNA transfection and silencing of RRM2 by siRRM2 in these STS cell lines, the RRM2 expression levels were analyzed by Western blot.

RESULTS: We observed a direct correlation between viral oncolysis and RRM2 mRNA levels ($R = 0.96$) in STS. Higher RRM2 expression was associated with a more robust cell kill. Silencing the RRM2 gene led to significantly greater cell survival (80%) compared with the control group ($P = .003$), whereas overexpression of the RRM2 increased viral oncolysis by 33% ($P < .001$).

CONCLUSIONS: Our results show that the oncolytic effects of MYXV correlate directly with RR expression levels and are enhanced in STS cell lines with naturally occurring or artificially induced high expression levels of RR. Myxoma virus holds promise in the treatment of advanced soft tissue cancer, especially in tumors overexpressing RR.

KEYWORDS: Soft tissue sarcoma, myxoma virus, ribonucleotide reductase, biomarker, oncolytic viral therapy

RECEIVED: May 12, 2020. **ACCEPTED:** January 15, 2021.

TYPE: Original Article

FUNDING: The author(s) disclosed receipt of the following financial support for the research, authorship, and/or publication of this article: This work was supported in part by the National Institutes of Health (R01CA75416; Y.F); Mr William H. Goodwin and Mrs Alice Goodwin and the Commonwealth Foundation for Cancer Research grant—The Experimental Therapeutics Center of Memorial Sloan Kettering Cancer Center (Y.F); and the Soft Tissue Sarcoma Program Project (P01CA047179; S.S.).

DECLARATION OF CONFLICTING INTERESTS: The author(s) declared no potential conflicts of interest with respect to the research, authorship, and/or publication of this article.

CORRESPONDING AUTHOR: Yuman Fong, Department of Surgery, City of Hope National Medical Center, Malp Building 182, 2nd floor, 2207, 1500 East Duarte Road, Duarte, CA 91010, USA. Email: yfong@coh.org

Introduction

Oncolytic virotherapy is a promising anticancer strategy that exploits either naturally occurring or genetically engineered viral tropism for cancer cells. In 2015, the Food and Drug Administration-approved talimogene laherparepvec (Amgen Inc), an immuno-oncolytic herpes simplex virus engineered to secrete the immunostimulatory protein granulocyte-macrophage colony-stimulating factor for advanced melanoma, became the first clinically successful immuno-oncolytic virotherapy.[1] Several other oncolytic viruses (OVs) such as adenovirus, herpes simplex virus, Newcastle disease virus, vaccinia virus, and reovirus have demonstrated encouraging preclinical results and show safety and promise in clinical trials for the treatment of solid tumors.[2] However, few studies have shown the efficacy of OVs in the treatment of soft tissue sarcomas (STS).

Myxoma virus (MYXV) is a large dsDNA poxvirus[3] that has demonstrated oncolytic activity against various malignancies, including acute myeloid leukemia, multiple myeloma, pancreatic cancer, glioma, rhabdoid tumors, medullary blastoma, and melanoma more recently in large animal models of STS.[4-6] Interestingly, the MYXV genome lacks the gene for 1 of the 2 subunits of ribonucleotide reductase (RR). The functional complex of subunits RRM1 and RRM2 is responsible for DNA synthesis and cellular repair in mammalian cells. The absence of an RR subunit in the MYXV genome distinguishes MYXV from other orthopoxviruses such as vaccinia virus which possesses both RR components.[7] Studies have suggested

MYXV survival is hence more dependent on host cell metabolism enzymes and nucleotide pools in contrast to other oncolytic poxviruses.[3] In addition, this dependence suggests that MYXV may be more effective as a selective viral oncolytic agent in tumors with high RR levels such as some STS.[7]

Soft tissue sarcomas make up less than 1% of all solid malignancies and are projected to take 5150 lives in 2019 in the United States.[8] High-grade STS are especially difficult to treat with greater rates of local and distant recurrences after complete resections.[9-11] Liposarcoma and synovial sarcomas are the most common histologic subtypes of STS, accounting for ⩾30% of all adult sarcomas.[12] The limitations of surgical resection and the ineffectiveness of additional systemic and regional treatments for these aggressive malignancies challenge investigators to discover more sophisticated and potent immunooncolytic agents.

Our study investigates MYXV as a potential therapeutic agent against STS along with the role of host cell *RRM2* expression levels in its anticancer efficacy. We hypothesize that MYXV relies on host cell *RRM2* levels to kill infected cancer cells and the oncolytic efficacy is greater in STS with high *RRM2* expression compared with lower *RRM2* expressing STS and normal adipose tissue. We demonstrate for the first time the oncolytic effects of MYXV against human liposarcoma and synovial sarcoma in vitro. The results provide supporting evidence for the importance of the endogenous expression levels of *RRM2* for MYXV in targeting cancer cells.

Materials and Methods

Cell lines

Human STS cell lines LS141 (a dedifferentiated liposarcoma), DDLS8817 (a dedifferentiated liposarcoma), RDD2213 (recurrent dedifferentiated liposarcoma), and HSSYII (a synovial sarcoma) derived from human tumor samples and maintained as previously described[12] were grown to 70% to 80% confluency in T225 flasks in a humidified incubator (37°C, 5% CO_2). The genotype and phenotype of the cells were validated and confirmed to be mycoplasma negative before experimental use. All in vitro studies using human cell lines were approved by the institutional review board (IRB) of Memorial Sloan Kettering Cancer Center (IRB protocol 02-060). Cells from the same flask were used for each unit of the experiments that included cytotoxicity assays, RNA isolation for cDNA synthesis followed by quantitative real-time polymerase chain reaction (qRT-PCR), and protein isolation. Baby green monkey kidney (BGMK) cells were acquired from Dr Grant McFadden laboratory (Gainesville, FL) and maintained in Dulbecco's modified Eagle's medium 10% fetal calf serum (FCS) for viral titering.

Myxoma virus, vMyx-GFP

vMyx-GFP, a replication-competent, genetically engineered virus derived from the Lausanne strain which has a gene insertion for enhanced green fluorescent protein (eGFP) between open reading frames M135R and M136R of its genome was used. On infection of a host cell, the expression of eGFP is regulated by a poxvirus synthetic early/late promoter. vMyx-GFP was titered on BGMK cells by counting focus-forming units (FFUs) under Carl Zeiss fluorescent filter microscope, Axiovert 2000M (Carl Zeiss Inc, Thornwood, NY). This microscope was also used to visualize virally infected cells by observing fluorescent expression of eGFP.

One-step viral proliferation assay

LS141, DDLS8817, RDD2213, and HSSYII cells were plated in 6-well flat-bottom plates with 2 mL of growth media. After cell attachment and 80% to 95% of confluency, media was removed and the cells were infected with vMyx-GFP at a multiplicity of infection (MOI) of 3 in a volume of 0.5 mL. At time points of 0, 4, 24, and 48 hours after viral infection, cells were collected and viral particles were released by the freeze-thaw process. Meanwhile, BGMK cells were plated to 90% confluency in 24-well plates. The respective lysates for different cell lines at the indicated time points were inoculated into the BGMK cells and incubated at room temperature for 1 hour. After an hour of incubation, FFUs were counted using a Carl Zeiss fluorescent filter microscope, Axiovert 200M.

Cytotoxicity assay

LS141, HSSYII, DDLS8817, and RDD2213 were plated in 12-well flat-bottom plates and infected with vMyx-GFP at MOIs of 0.1, 1, or 10 in triplicate. On days 1, 3, 5, and 7 after infection, cells were washed with phosphate-buffered solution and lysed with 1.35% Triton-X to release intracellular lactate dehydrogenase (LDH). The amount of LDH released in the lysate of the infected tumor cells was compared with that of uninfected tumor cells to determine the cytotoxic effect of viral infection. The amount of LDH per well was quantified using a Cytotox 96 nonradioactive cytotoxicity assay (Promega, Madison, WI) by measuring the absorbance of color change with the conversion of tetrazolium salt into a formazan product. Absorbance was measured at 450 nm using a microplate reader (EL 312e: BioTek Instruments, Winooski, VT). Results were expressed using the survival of infected cells as a percent of control untreated cells.

RNA isolation and cDNA synthesis

Cells were harvested at 70% to 90% confluency and RNA was isolated using the RNeasy Mini-Kit (Qiagen, Valencia, CA) as described by the manufacturer. A 20-gauge needle was used to homogenize the cells during lysis. While isolating the RNA, optional on-column digestion was performed with the RNase-Free DNase Set (Qiagen) as described by the manufacturer to provide improved RNA purity and yield. Reverse transcription polymerase chain reaction was performed with 1.5 µg of RNA

in a 100-μL reaction using random hexamer priming and TaqMan Reverse Transcription Reagents (Applied Biosystems, Foster City, CA) on a Thermo Hybrid thermocycler (Waltham, MA).

Quantitative real-time PCR (qRT-PCR)

qRT-PCR was performed on an ABI PRISM 7900 HT Sequence Detection System (Applied Biosystems) with TaqMan Assays-on-Demand Gene Expression assay primers for *RRM2* and 18s rRNA. The data from the sequencing were analyzed using SDS Version 2.1 software (Applied Biosystems). The conditions for qRT-PCR were as follows: step 1, 48°C for 30 minutes; step 2, 95°C for 10 minutes; and step 3, 40 cycles at 95°C for 15 seconds, and 60°C for 1 minute. The amount of *RRM2* RNA expression in each sample was calculated based on the standard curve generated with the RNA from LS141 cells, known to express the highest relative amount of *RRM2*. The *RRM2* expression data were normalized to an endogenous control gene, the 18s rRNA as described in User Bulletin #2 (Applied Biosystems). The normalized value for each cell line was compared with *RRM2* expression of normal fat and expressed as a fold-increase from normal preadipocyte expression.

Small interfering (siRNA) transient transfection

siRNA for *RRM2* and a nontargeting pool were obtained from Dharmacon, Inc (Lafayette, CO). The sense sequence of the small inhibitory RR subunit 2 (siRRM2) strand was 5′-GGAGUGAUGUCAAGUCCAAUU-3′. The antisense sequence was 5′-UUGGACUUGACAUCACCUU-3′. LS141 cells were plated at 2E4 cells per well in 12-well plates, and 3E5 cells per well in 6-well plates. Oligofectamine transfection reagent (Invitrogen, Carlsbad, CA) was optimized at a concentration of 3 μL of reagent to 8 μL of media with 5 μL of 20 μM siRRM2 in a total of 85 μL of media per well of a 12-well plate. Samples were plated in triplicate, and identical concentrations were used for the si-nontargeting pool. For the cells plated at 60% to 80% confluency in 6-well plates, 5 μL of Oligofectamine in 10 μL of media was mixed with 10 μL of 20-μM siRRM2 in 175 μL of media for transfection optimization. Fetal calf serum and antibiotics were reintroduced to the cells after 4 hours in FCS and antibiotic-free media. At 48, 72, 120, and 168 hours after transfection, the cells in 6- and 12-well plates were collected for Western blot analysis to evaluate for the effectiveness of siRRM2.

Plasmid cDNA transient transfection

The plasmid containing cDNA for RRM2 was a generous contribution from Dr B. Zhou at the City of Hope Comprehensive Cancer Center (Duarte, CA). Plasmid cDNA RRM2 was verified using a diagnostic restriction digest and was amplified along with the empty vector using the MaxiPrep Kit according to manufacturer instructions (Qiagen). Transient transfection of plasmids was performed using the lipid reagent gene porter (Gene Therapy Systems, Inc, San Diego, CA) according to manufacturer instructions. 1E6 DDLS8817 cells were seeded in 6-well plates to reach 60% to 80% of confluency overnight. Ph-beta-Apr-1-neo control (4 μg) and ph-beta-Apr-1-neo containing RRM2 (4 μg) plasmids were transfected in serum- and antibiotic-free media. Cells were collected after 48 hours and 7 days following transfection, and protein was extracted for RRM2 analysis by Western blot. The remainder of the cells were plated and allowed to proliferate to 80% confluency in a T225 flask. Neomycin was used to select neomycin-resistant transfected colonies. These cells were passaged 3 times before Western blot analysis and LDH cytotoxicity experiments were conducted. RRM2 plasmid cDNA-transfected cells and those with empty vector transfection were used for cytotoxicity analysis.

Western blot

Endogenous RRM2 protein levels were assessed by collecting a cell pellet from the same flask used to plate for the cytotoxicity assay. Protein extracts of 20 μg each were run on 10% Tris-glycine-sodium dodecyl sulfate gels (Bio-Rad), transferred to a polyvinylidene difluoride membrane, and probed for RRM2. Primary antibodies for RRM2 were chicken anti-RRM2 (N-92 and polyclonal IgY horseradish peroxidase [HRP]; GenWay Biotech, San Diego, CA). The secondary antibody used for RRM2 was goat anti-chicken IgY Fc fragment, HRP conjugate (1:10 000). α-tubulin was also probed (Santa Cruz Biotechnology, Inc Santa Cruz, CA).

Statistical analysis

All in vitro experiments were performed at least 3 times, and samples were plated and run in triplicate. Results are expressed as means ± SEM. Student *t* tests were used to compare 2 groups, and *P* values $<.05$ were considered statistically significant.

Results

Myxoma virus infects and kills human STS cells

It was observed that vMyx-GFP (an MYXV construct that constitutively expresses eGFP under poxvirus synthetic early/late promoter) effectively kills a panel of human STS cell lines. Myxoma virus infection of LS141, HSSYII, DDLS8817, and RDD2213 cells at an MOI of 10 was confirmed by examination of eGFP expression in infected cells within 24 hours (Figure 1).

Myxoma virus efficiently infected human STS cell lines by displaying rapid and logarithmic replication within 48 hours of infection. Representative experiments are shown in a one-step viral proliferation curve (Figure 2). Cell viability assays after MYXV infection showed that LS141 was the most sensitive

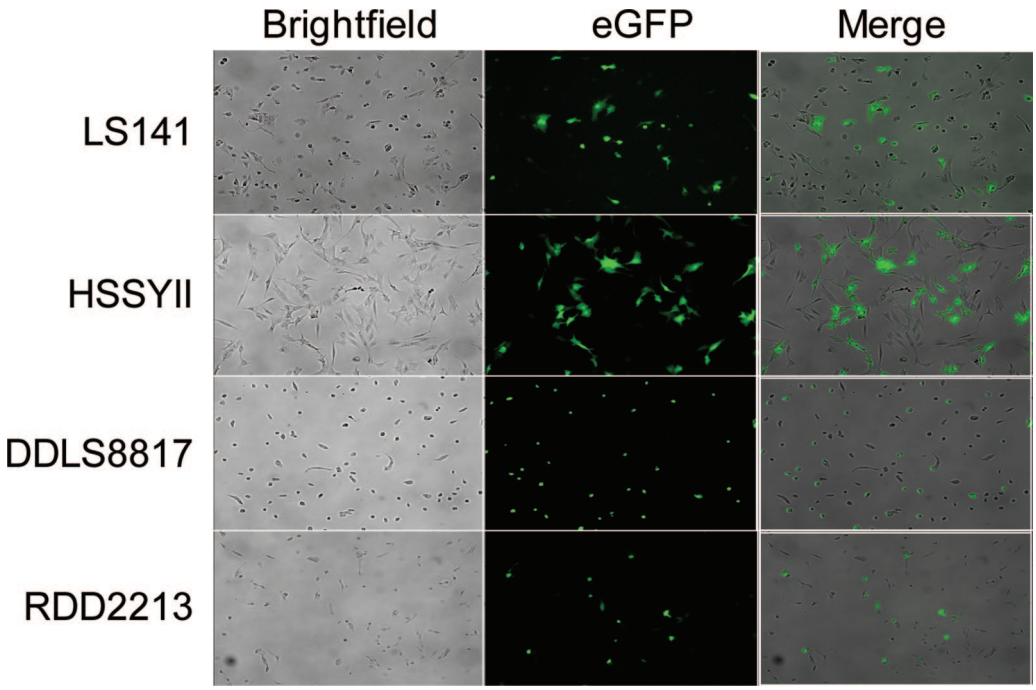

Figure 1. Soft tissue sarcoma cell lines express eGFP 24 hours after infection with vMyx-GFP at an MOI of 10. Four STS cell lines—LS141 (a dedifferentiated liposarcoma), DDLS8817 (a dedifferentiated liposarcoma), RDD2213 (recurrent dedifferentiated liposarcoma), and HSSYII (a synovial sarcoma)—were infected with vMyx-GFP at an MOI of 10. After 24 hours of infection, they were visualized using fluorescence and brightfield microscopy. The first column represents brightfield imaging of the 4 cell lines demonstrating the morphology of the cells (100× magnification). The second column represents areas of eGFP expression detected under fluorescence that correspond to vMyx-GFP-infected sarcoma cells as demonstrated by overlay images in the third column.
eGFP indicates enhanced green fluorescent protein; MOI, multiplicity of infection; STS, soft tissue sarcoma.

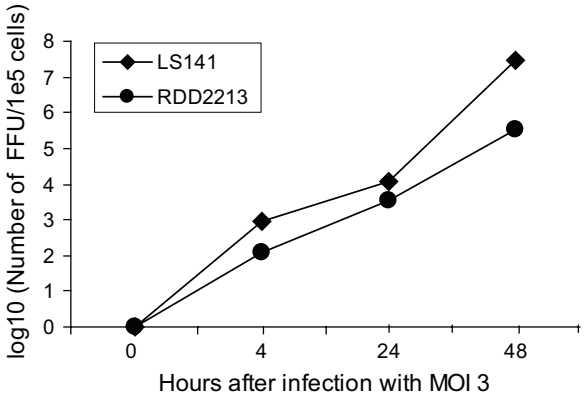

Figure 2. Soft tissue sarcoma cells permit exponential replication of the MYXV. Representative sarcoma cell lines—LS141 (a dedifferentiated liposarcoma) and RDD2213 (recurrent dedifferentiated liposarcoma)—were infected with vMyx-GFP at an MOI of 3, and then collected to evaluate the number of viral FFUs at 0, 4, 24, and 48 hours after infection.
FFUs indicates focus-forming units; MOI, multiplicity of infection; MYXV, myxoma virus.

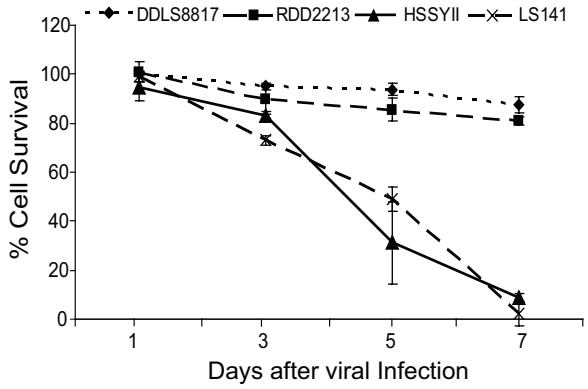

Figure 3. Sensitivity of sarcoma cell lines to MYXV oncolysis at an MOI of 10. Sarcoma cell lines—LS141 (a dedifferentiated liposarcoma), DDLS8817 (a dedifferentiated liposarcoma), RDD2213 (recurrent dedifferentiated liposarcoma), and HSSYII (a synovial sarcoma)—were infected with MYXV at an MOI of 10 and analyzed for percent cell survival compared with control nontreated cells on days 1, 3, 5, and 7 with LDH cytotoxicity assays.
LDH indicates lactate dehydrogenase; MOI, multiplicity of infection; MYXV, myxoma virus.

cell line with 97.81% ± 4.94% cells killed, followed by HSSYII with 91.25% ± 1.62% cells killed at day 7 with an MOI of 10. However, DDLS8817 and RDD2213 cell lines were resistant to MYXV killing with 87.65% ± 3.21% and 81.00% ± 1.60% cells still viable on day 7 following infection at an MOI of 10, respectively (Figure 3).

Endogenous levels of RRM2 in human STS cell lines correlate with MYXV cytotoxicity of these cell lines

Endogenous *RRM2* mRNA expression levels in sarcoma cell lines were measured by qRT-PCR. A direct correlation between cell survival and endogenous levels of *RRM2* was

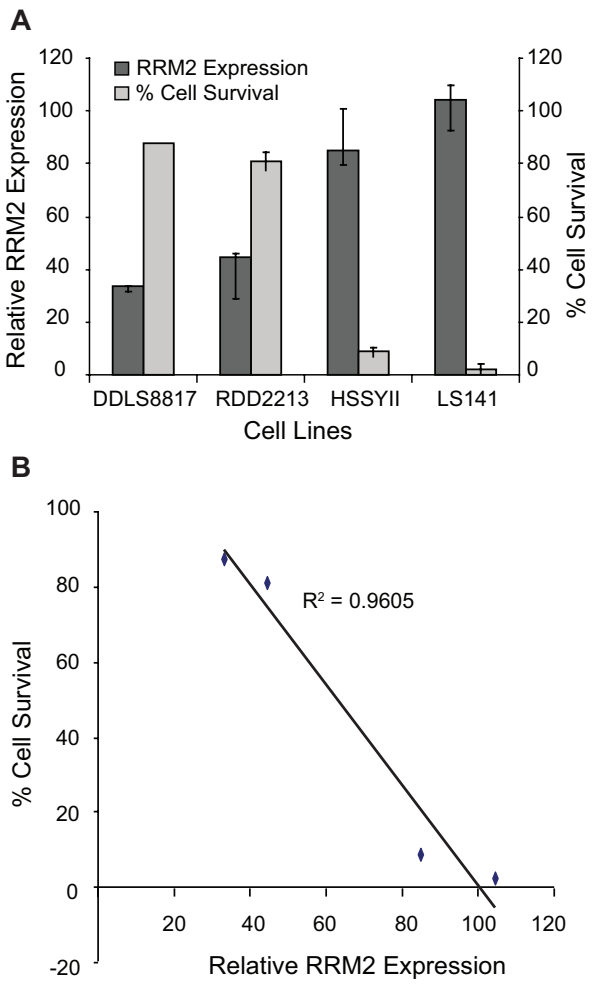

Figure 4. Increased viral cytotoxicity correlates with increased *RRM2* expression in STS cells. (A) The relative *RRM2* expression levels in sarcoma cell lines as compared with normal fat are represented here as solid gray bars from lowest to highest: LS141 (104×; a dedifferentiated liposarcoma), HSSYII (85×; a synovial sarcoma), RDD2213 (45×; recurrent dedifferentiated liposarcoma), and DDLS8817 (33×; a dedifferentiated liposarcoma). The corresponding percent cell survival on day 7 is shown in light gray bars. (B) Percent cell survival on day 7 after viral infection is plotted against endogenous *RRM2* mRNA expression levels. The graph demonstrates a strong inverse correlation of *RRM2* levels and cell survival with Pearson coefficient of 0.9605.
RRM2 indicates ribonucleotide reductase subunit 2; STS, soft tissue sarcoma.

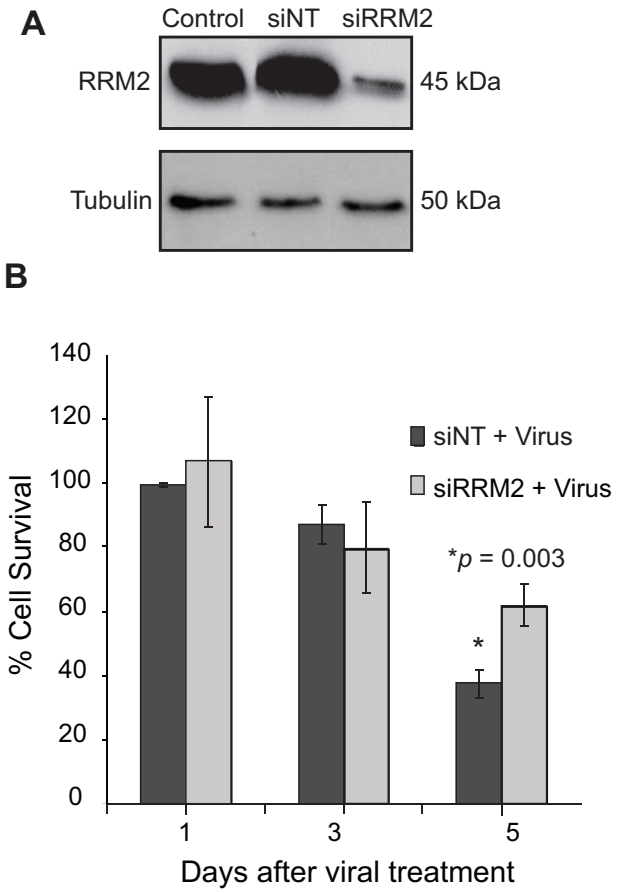

Figure 5. Decreased RRM2 protein levels lead to lower viral oncolysis in the STS cell line LS141. (A) siRNA-directed knockdown of *RRM2* is demonstrated by a representative Western blot analysis 72 hours following siRRM2 transfection. Effective suppression of *RRM2* is achieved in the knockdown cells as opposed to the control and nontargeted (siNT) pool-transfected cells, which maintained high expression of *RRM2*. (B) After 48 hours of transfection, cells were infected with MYXV at an MOI of 10. On day 5 after viral infection, the siRRM2 transfected cells showed 25% greater cell survival, compared with cells with nontargeted transfections ($P = .003$).
MOI indicates multiplicity of infection; MYXV, myxoma virus; RRM2, ribonucleotide reductase subunit 2; siRRM2, small inhibitory ribonucleotide reductase subunit 2; STS, soft tissue sarcoma.

observed following MYXV infection of LS141, HSSYII, RDD2213, and DDLS8817 cells (Figure 4A). The 2 highest *RRM2*-expressing cell lines were LS141 and HSSYII with 104- and 85-fold relatively higher mRNA levels compared with baseline expression in normal preadipocytes, respectively (Figure 4A). These high-*RRM2*-expressing cell lines were also the most sensitive to MYXV infection. In contrast, DDLS8817 and RDD2213 cell lines demonstrated a 33- and 45-fold higher *RRM2* mRNA level over the baseline making them comparatively low-*RRM2*-expressing sarcoma cell lines, respectively. DDLS8817 and RDD2213 cell lines were less sensitive to MYXV infection. A strong inverse correlation between *RRM2* mRNA expression and cell survival after viral infection was observed as indicated by Pearson coefficient of 0.96 (Figure 4B).

siRNA-mediated knockdown of RRM2 decreased MYXV cytotoxicity in LS141 cell line

We tested the functional effect of RRM2 on the ability of MYXV to cause oncolysis in STS cell lines. *RRM2* was significantly downregulated with siRNA in LS141, the cell line with the highest levels of *RRM2* expression. Downregulation of RRM2 protein expression was confirmed by Western blot analysis (Figure 5A). Next, we compared cell viability at days 1, 3, and 5 after MYXV infection of LS141 cells transfected with siRRM2 with the nontargeting control siRNA (siNTC) transfected cells. On day 5 after viral infection, a significant difference in the cellular sensitivity to MYXV-induced oncolysis was

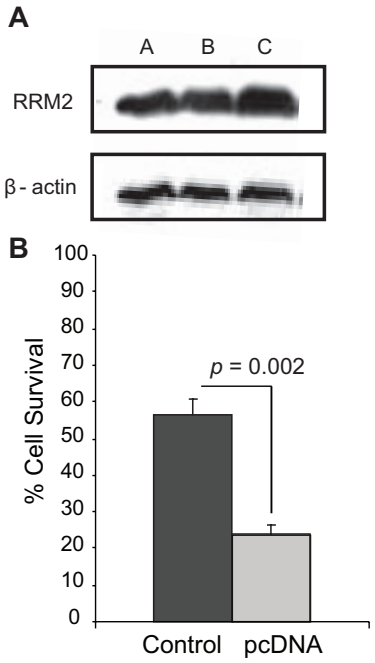

Figure 6. Enhanced expression of *RRM2* in DDLS8817 (a dedifferentiated liposarcoma) cells increased MYXV oncolysis. (A) Representative Western blot showing upregulation of RRM2 in low-*RRM2*-expressing DDLS8817 cells following transfection of a plasmid expressing RRM2 (pcDNA-RRM2). Column A represents protein collected from cells 7 days after empty vector transfection. Column B represents protein collected from cells 2 days after pcDNA-RRM2 vector transfection. Column C represents protein collected 7 days after pcDNA-RRM2 vector transfection demonstrating ~50% upregulation. (B) Lactate dehydrogenase cytotoxicity data for DDLS8817 cells transfected with either the control vector or pcDNA-RRM2 on day 7 postinfection with MYXV. pcDNA-RRM2 transfected cells demonstrate a 33% increased sensitivity to MYXV as compared with control cells.
MYXV indicates myxoma virus; pcDNA-RRM2, plasmid construct DNA; RRM2, ribonucleotide reductase subunit 2.

observed with 62% live siRRM2 transfected cells versus 37% of live siNTC cells ($P = .003$; Figure 5B).

Overexpression of RRM2 in endogenously low-RRM2-expressing cell lines sensitizes them to MYXV-induced oncolysis

We then tested whether overexpression of *RRM2* sensitizes cell lines with lower levels of endogenous *RRM2* to MYXV-induced oncolysis. The low-*RRM2*-expressing DDLS8817 cell line was successfully transfected with a plasmid expressing *RRM2* (pcDNA-RRM2). Densitometric analysis following Western blot analysis revealed 50% upregulation of RRM2 protein expression on day 7 after the transfection of pcDNA-RRM2, compared with the empty vector-transfected cells (Figure 6A). On day 7 following infection of these cells with MYXV, a significant increase in oncolysis ($P = .002$) was observed in pcDNA-RRM2 transfected cells compared with cells transfected with the control plasmid (Figure 6B). These results indicate that overexpression of *RRM2* in cell lines with low levels of endogenous *RRM2* increased their sensitivity to MYXV-induced oncolysis.

Discussion

In this study, we demonstrate for the first time that MYXV infects and kills human liposarcoma and synovial sarcoma cell lines. *RRM2* expression levels in these sarcoma cell lines directly correlated with MYXV-induced cytotoxicity. Knockdown of *RRM2* levels with RNA interference in STS cells with high *RRM2* levels reduced the cytotoxic effects of MYXV infection, whereas upregulation of *RRM2* in a human STS cell line expressing low levels of *RRM2* enhanced MYXV cytotoxicity. These results strongly suggest that RRM2 activity is intimately associated with the ability of MYXV to infect and kill these cells.

Ribonucleotide reductase is a heterodimeric enzyme complex that catalyzes the formation of deoxyribonucleotides from ribonucleotides. The inhibition of either of the 2 RR subunits, large subunit (RRM1) or small subunit (RRM2), impairs DNA replication and causes replication stress in normal and cancer cells.[13] While both subunits are transcribed during the S-phase of the cell cycle, RRM1 has a longer half-life of 15 hours, whereas RRM2 has a relatively short half-life making this subunit the rate-limiting protein. Overexpression of *RRM2* in cancer cells has been implicated in the progression of several solid tumors, including lung, breast, colorectal, neuroblastoma, and STS.[14-17] Mechanistically, overexpression of RR has been implicated in promoting tumor invasiveness.[18-20] Targeting pathways that upregulate or downregulate *RRM2* expression levels offer the potential to alter tumor growth and to improve treatment response.[21-24]

A limitation of this study is the lack of in vivo experiments. It is not known whether RRM2 activity will be as important in animal models of STS. However, we do know from previous animal studies that MYXV is safe and effective in large animal models of STS. In a canine model that spontaneously develops STS, animals treated with intratumoral injection of a genetically modified MYXV with a deletion of the *serp2* gene (MYXVΔserp2), no detrimental effects were observed in any of these canine subjects.[6] In addition, the exclusive tropism of MYXV for human cancer cells versus normal cells has been associated with key abnormal cell signaling pathways such as dysfunctional protein kinase B (Akt), protein kinase R, sterile alpha motif domain containing 9, and various host DEAD-box RNA helicases which are involved in cancer cell selectivity and antitumor activity of MYXV. Previous work established that MYXV is dependent on the basal level of phosphorylated Akt,[25] and combination with drugs such as rapamycin increases Akt phosphorylation and enhances MYXV antitumor activity in gallbladder cancer and medulloblastoma.[26] Moreover, intratumoral treatment of subcutaneous xenografts of human embryonic rhabdomyosarcoma in NSG mouse models with wild-type MYXV and NRAS (neuroblastoma RAS viral oncogene

homolog) targeting CRISPR-cas9 engineered MYXV reduced tumor volume and prolonged mouse survival.[27] Such studies demonstrate the safety of a genetically modified version of MYXV in vivo and support the advancement of MYXV constructs into human clinical trials.

Overall, our results showing that *RRM2* expression levels correlate with MYXV oncolytic efficacy expand the body of knowledge of MYXV's oncolytic potential to include human liposarcoma and synovial sarcoma. The robust oncolytic activity of MYXV observed in human STS cell lines expressing the highest levels of *RRM2* also reveals that endogenous *RRM2* levels could be used as a potential biomarker to predict response rates to this oncolytic agent. Moreover, *RRM2* levels could also guide patient selection in clinical trials in STS and other cancers with high *RRM2* expression. Importantly, our results suggest that therapeutic strategies manipulating cellular levels of RR in target cancer cells could render otherwise unresponsive tumor cells susceptible to oncolytic virotherapy with MYXV and broaden the scope of immunotherapy for STS.

Acknowledgements

The authors thank Indra M. Newman, PhD, and Supriya Deshpande, PhD for manuscript editing assistance.

Author Contributions

Study concept and design (YF, YW, GM), Acquisition of data (YW, SW, RG, PD), Analysis and interpretation of data (YW, PD, MS, RM, SS, GM, YF), Drafting of the manuscript (YW, SW, PD, RM), Critical revision (YW, SW, RG, PD, MS, RM, SS, GM, YF). All authors read and approved the final manuscript.

ORCID iD

Yuman Fong https://orcid.org/0000-0002-8934-9959

REFERENCES

1. Andtbacka RH, Kaufman HL, Collichio F, et al. Talimogene laherparepvec improves durable response rate in patients with advanced melanoma. *J Clin Oncol*. 2015;33:2780-2788.
2. Warner SG, O'Leary MP, Fong Y. Therapeutic oncolytic viruses: clinical advances and future directions. *Curr Opin Oncol*. 2017;29:359-365.
3. Cameron C, Hota-Mitchell S, Chen L, et al. The complete DNA sequence of myxoma virus. *Virology*. 1999;264:298-318.
4. Chan WM, Rahman MM, McFadden G. Oncolytic myxoma virus: the path to clinic. *Vaccine*. 2013;31:4252-4258.
5. Sypula J, Wang F, Ma Y, Bell J, McFadden G. Myxoma virus tropism in human tumor cells. *Gene Ther Mol Biol*. 2004;8:103-114.
6. MacNeill AL, Weishaar KM, Seguin B, Powers BE. Safety of an oncolytic myxoma virus in dogs with soft tissue sarcoma. *Viruses*. 2018;10:398.
7. Gammon DB, Gowrishankar B, Duraffour S, Andrei G, Upton C, Evans DH. Vaccinia virus-encoded ribonucleotide reductase subunits are differentially required for replication and pathogenesis. *PLoS Pathogens*. 2010;6:e1000984.
8. Society AC. *Cancer Facts and Figures*. Atlanta, GA: American Cancer Society; 2018.
9. Lewis JJ, Antonescu CR, Leung DH, et al. Synovial sarcoma: a multivariate analysis of prognostic factors in 112 patients with primary localized tumors of the extremity. *J Clin Oncol*. 2000;18:2087-2094.
10. Singer S, Antonescu CR, Riedel E, Brennan MF. Histologic subtype and margin of resection predict pattern of recurrence and survival for retroperitoneal liposarcoma. *Ann Surg*. 2003;238:358-370; discussion 370-351.
11. Eilber FC, Eilber FR, Eckardt J, et al. The impact of chemotherapy on the survival of patients with high-grade primary extremity liposarcoma. *Ann Surg*. 2004;240:686-695; discussion 695-687.
12. Singer S, Socci ND, Ambrosini G, et al. Gene expression profiling of liposarcoma identifies distinct biological types/subtypes and potential therapeutic targets in well-differentiated and dedifferentiated liposarcoma. *Cancer Res*. 2007;67:6626-6636.
13. Nordlund P, Reichard P. Ribonucleotide reductases. *Annu Rev Biochem*. 2006;75:681-706.
14. Liu X, Zhou B, Xue L, et al. Ribonucleotide reductase subunits M2 and p53R2 are potential biomarkers for metastasis of colon cancer. *Clin Colorectal Cancer*. 2007;6:374-381.
15. Zhu Z, Jin Z, Deng Y, et al. Co-expression network analysis identifies four hub genes associated with prognosis in soft tissue sarcoma. *Front Genet*. 2019;10:37.
16. Li J, Pang J, Liu Y, et al. Suppression of RRM2 inhibits cell proliferation, causes cell cycle arrest and promotes the apoptosis of human neuroblastoma cells and in human neuroblastoma RRM2 is suppressed following chemotherapy. *Oncol Rep*. 2018;40:355-360.
17. Wang L, Meng L, Wang XW, Ma GY, Chen JH. Expression of RRM1 and RRM2 as a novel prognostic marker in advanced non-small cell lung cancer receiving chemotherapy. *Tumour Biol*. 2014;35:1899-1906.
18. Zhou BS, Tsai P, Ker R, et al. Overexpression of transfected human ribonucleotide reductase M2 subunit in human cancer cells enhances their invasive potential. *Clin Exp Metastasis*. 1998;16:43-49.
19. Morikawa T, Hino R, Uozaki H, et al. Expression of ribonucleotide reductase M2 subunit in gastric cancer and effects of RRM2 inhibition in vitro. *Hum Pathol*. 2010;41:1742-1748.
20. Yan D, Wang W. [SATB1 promotes the malignant of human non-Hodgkin lymphoma by activating the ribonucleotide reductase small subunit M2]. *Zhong Nan Da Xue Xue Bao Yi Xue Ban / J Cent South Univ Med Sci*. 2016;41:1155-1162.
21. Das B, Roy J, Jain N, Mallick B. Tumor suppressive activity of PIWI-interacting RNA in human fibrosarcoma mediated through repression of RRM2. *Mol Carcinog*. 2019;58:344-357.
22. Liang WH, Li N, Yuan ZQ, Qian XL, Wang ZH. DSCAM-AS1 promotes tumor growth of breast cancer by reducing miR-204-5p and up-regulating RRM2. *Mol Carcinog*. 2019;58:461-473.
23. Wang A, Zhao C, Liu X, et al. Knockdown of TBRG4 affects tumorigenesis in human H1299 lung cancer cells by regulating DDIT3, CAV1 and RRM2. *Oncol Lett*. 2018;15:121-128.
24. Burton C, Das A, McDonald D, et al. Oncolytic myxoma virus synergizes with standard of care for treatment of glioblastoma multiforme. *Oncolytic Virother*. 2018;7:107-116.
25. Wang G, Barrett JW, Stanford M, et al. Infection of human cancer cells with myxoma virus requires Akt activation via interaction with a viral ankyrin-repeat host range factor. *Proc Natl Acad Sci USA*. 2006;103:4640-4645.
26. Weng M, Gong W, Ma M, et al. Targeting gallbladder cancer: oncolytic virotherapy with myxoma virus is enhanced by rapamycin in vitro and further improved by hyaluronan in vivo. *Mol Cancer*. 2014;13:82.
27. Phelps MP, Yang H, Patel S, Rahman MM, McFadden G, Chen E. Oncolytic virus-mediated RAS targeting in rhabdomyosarcoma. *Mol Ther Oncolytics*. 2018;11:52-61.